

# Hubbard-like Hamiltonian for ultracold atoms in a one-dimensional optical lattice

Francesco Massel and Vittorio Penna

*Dipartimento di Fisica and UdR INFM, Torino Politecnico, Corso Duca degli Abruzzi 24, I-10129 Torino, Italy*

(Received 1 April 2005; revised manuscript received 27 July 2005; published 17 November 2005)

Based on the standard many-fermion field theory, we construct models describing ultracold fermions in a one-dimensional optical lattice by implementing a mode expansion of the fermionic field operator where modes, in addition to space localization, take into account the quantum numbers inherent in local fermion interactions. The resulting models are generalized Hubbard Hamiltonians whose interaction parameters are derived by a fully analytical calculation. The special interest for this derivation resides in its model-generating capability and in the flexibility of the trapping techniques that allow the tuning of the Hamiltonian interaction parameters over a wide range of values. While the Hubbard Hamiltonian is recovered in the very low-density regime, in general, far more complicated Hamiltonians characterize high-density regimes, revealing a rich scenario for both the phenomenology of interacting trapped fermions and the experimental realization of devices for quantum-information processing. As a first example of the different situations that may arise beyond the models well known in the literature (the unpolarized-spin fermion model and the noninteracting spin-polarized fermion model), we derive a rotational Hubbard Hamiltonian describing the local rotational activity of spin-polarized fermions. Based on standard techniques we obtain the mean-field version of our model Hamiltonian and show how different dynamical algebras characterize the cases of attractive and repulsive two-body potentials.

DOI: [10.1103/PhysRevA.72.053619](https://doi.org/10.1103/PhysRevA.72.053619)

PACS number(s): 03.75.Ss, 71.10.Fd, 05.30.Fk

## I. INTRODUCTION

Since the Bose-Einstein condensation (BEC) of alkali-metal atoms in magnetic traps [1,2], a massive experimental and theoretical effort has been dedicated to the investigation of confined atoms in the extremely low-temperature regime (for a review see [3–6]).

The flexibility of optical trapping techniques has suggested devising different configurations (lattices [5,7–10], superlattices, etc. [11–16]), opening a vast scenario of research. The ability to tune atomic interactions via a magnetic field (Feshbach resonance [17]), along with the proposal of single-atom trap loading techniques [18], has proven to be of capital importance for ultracold fermions physics, yielding the possibility to study fundamental aspects of superfluidity (the BCS-BEC crossover; see, e.g., [19–22]) and envisaging additional perspectives in quantum-information processing [23,24].

The present work focuses on the theoretical investigation of the properties of (few) fermionic ultracold atoms loaded into a one-dimensional (1D) optical lattice, where global confinement is ensured by a magnetic trap.

We have here considered an experimental setup with tunable lattice constant and barrier height (see Fig. 1).

The description of such a physical system can be naturally performed in terms of a generalized Hubbard Hamiltonian (GHH) which is deduced from a general field-theoretic Hamiltonian with two-body interaction [25]. At this stage, particular care must be taken in the choice of the function basis for the field operator expansion. Although the symmetries of the system can provide selection rules that reduce the involvement of the GHH, the resulting coefficient structure is very rich and, as a direct consequence, the Hamiltonian is hardly tractable. Nevertheless, the generality of the model gives rise to a wealth of submodels, depending upon differ-

ent approximations and regimes. The guideline to find simplified Hamiltonians is given by a thorough analysis of the GHH coefficient structure.

From this perspective the analytical knowledge of the coefficients is a powerful tool to establish the physical relevance of different submodels in the various situations that may be conceived in the framework of trapped-ultracold-atom physics. Moreover, the nontrivial dependence of the coefficient on adjustable external parameters provides the possibility of using these parameters to control the dynamics of the atoms trapped in the optical lattice. Thus the key aspect of this paper is the analytical determination of the hopping and interaction coefficients as a function of experimental parameters such as magnetic trap frequency, laser

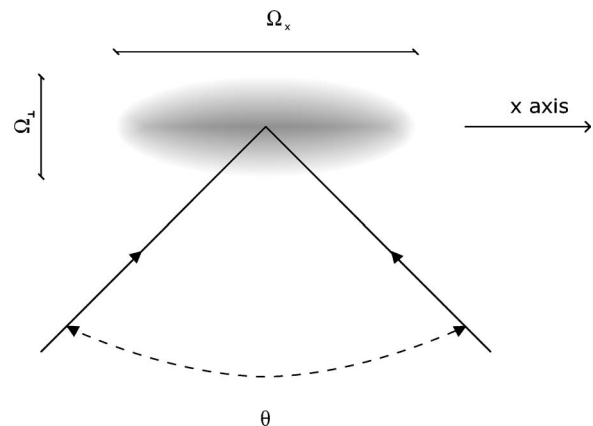


FIG. 1. Sketch of the experimental setup considered. Two laser beams at an angle  $\theta$  form an interference pattern within the fermionic cloud magnetically trapped with trapping frequencies  $\Omega_\perp$  and  $\Omega_x$ . The lattice constant can be tuned by adjusting the angle  $\theta$  according to the relation  $d = \lambda / [2 \sin(\theta/2)]$ .

intensity, wavelength, angle between laser sources,  $s$ -wave scattering length etc.

We would like to stress that the procedure followed here for the determination of the coefficients is statistics independent: the bosonic or fermionic nature of the atoms loaded into the trap is completely taken into account by the commutators of raising and lowering operators that will be described in the paper. For example, with the calculations performed here it seems feasible to go beyond the approximations that lead to the Bose-Hubbard model in the description of the BEC dynamics in optical lattices, taking into account the specific nature of the interaction between alkali-metal atoms in the low-density regime. Even for a ground-state calculation it can be shown that it is necessary to include levels beyond the single-particle ground state (see [26]).

The confinement model considered here has a direct experimental relevance (see, e.g., [27,28]). However, while in [27,28] a number of atoms of the order of  $10^4$  is considered, allowing thus the adoption of a semiclassical model, we focus on a low-occupation-number regime similarly to what is done in [29,30], yet extending to a multiband model whose correctness is limited by the validity limit of the space-mode approximation.

Challenging tasks for the future will include the determination of tractable yet interesting models for different aspects for theoretical condensed matter physics and quantum mechanics. On the other hand the experimental realization of systems that exhibit a behavior which can be described in the framework of the various models here proposed would represent an important achievement for both condensed matter experimentalist and theoreticians: the main difficulties seem to arise from the nearly-single-atom trap loading. In this situation the usual trap losses, due to heating engendered by laser detuning and quantum-diffractive background gas collisions [31], may play a significant role.

Throughout the paper we have tried to emphasize the generality of the procedure followed. However, we have decided to write down and plot a few numerical values of the coefficients to stress the fact that this calculation is a direct and relatively simple tool to shape out simplified and approximate Hamiltonians for different physical situations.

In Sec. II we depict the potential configuration of the system, moving then to the description of our field-theoretical approach. The field operators are written in terms of mode raising and lowering operators. Each mode corresponds to a set of quantum numbers; one of them identifies the lattice site (hence space-mode approximation) while the others describe on-site quantum numbers (local mode)[32]. As previously stated this choice is not unique, but symmetry constraints suggest expansions that emphasize conservation laws and selection rules.

In Sec. III we evaluate the expression of the Hamiltonian hopping and interaction coefficients and we try to describe the interaction coefficient symmetry properties in some detail.

The purpose of Sec. IV is twofold. On the one hand we show how, with suitable approximations, the Hamiltonian of the system reduces to known cases, such as the Hubbard Hamiltonian or a trivial noninteracting Hamiltonian. On the other, we introduce the rotational Hubbard Hamiltonian, as

an example of the involvement of higher-order approximations. For this case, by means of established mean-field approaches [33,34], we suggest a possible path of research involving general group-theoretical procedures [34]. It will be shown that these procedures, even if the explicit solution for the ground state is not given, allow us to grasp interesting aspects of the physics of the model here discussed.

We have included two Appendixes where the relatively simple but lengthy calculations of the tunneling and interaction coefficients are provided explicitly. In Appendix A there are various plots of multilevel hopping parameters that supply a good example of the scenario that we are moving in and may constitute a good starting point for further investigation.

## II. FERMIONS TRAPPED IN 1D OPTICAL LATTICES

### A. General features

The general field-theoretic Hamiltonian (see, e.g., [25]) with two-body interaction can be written as

$$\hat{H} = \int d\mathbf{r} \hat{\Psi}^\dagger(\mathbf{r}) H_{1b}(\mathbf{r}) \hat{\Psi}(\mathbf{r}) + \int d\mathbf{r} d\mathbf{r}' \hat{\Psi}^\dagger(\mathbf{r}) \hat{\Psi}^\dagger(\mathbf{r}') H_{2b}(\mathbf{r}, \mathbf{r}') \hat{\Psi}(\mathbf{r}') \hat{\Psi}(\mathbf{r}), \quad (1)$$

where  $H_{1b}(\mathbf{r})$  represents the one-body term of the Hamiltonian (kinetic+external potential term) while  $H_{2b}(\mathbf{r}, \mathbf{r}')$  is the two-body interaction potential term,  $\hat{\Psi}(\mathbf{r})$  is the field operator, and  $\hat{\Psi}^\dagger(\mathbf{r})$  is its adjoint.

As previously mentioned we will stick to neutral fermionic atoms loaded into a 1D optical lattice. We have taken into account a situation where the optical chain (laser wavelength  $\lambda=754$  nm) is loaded with  $^{40}\text{K}$  atoms. The barrier height in each point  $x$  is proportional to the intensity of the laser and thus, according to the considered setup, to  $\sin^2(2Kx)$  ( $K=\pi/d$  with  $d$  is lattice constant). For the evaluation of the multiplicative constant as a function of laser intensity, see, e.g., [3]. Here we set the multiplicative constant equal to  $m\omega^2/(2K^2)$  where  $\omega$  represents the harmonic oscillator frequency in the second-order expansion of the term  $V_{ext}$ . It is possible to express the barrier height in terms of recoil energy as  $V_0=sE_r$  with  $E_r=\hbar^2K^2/2m$  (see, e.g., [35]). In this arrangement there are then two control parameters for the tunneling coefficient,  $\theta$  and  $s$ . They both influence  $\omega_x$  and the lattice constant  $d$  according to the following equations:

$$d = \frac{\lambda}{2 \sin(\theta/2)}, \quad \omega_x = K\sqrt{2V_0/m}. \quad (2)$$

Global confinement is ensured by a cigar-shaped magnetic trap with principal axis along the  $x$  direction (see, e.g., [35]). This trap can be modeled by a 3D harmonic anisotropic trap of axial and radial frequencies equal to  $\Omega_x$  and  $\Omega_\perp$ , respectively ( $\Omega_x \ll \Omega_\perp$ ).

The magneto-optical trap can be thought of as if the constituents of the system were trapped in the cigar-shaped potential with a “slicing” effect of the laser, giving rise to a linear array of 3D prolate harmonic oscillators. In addition, the radial trapping frequency has a deep influence on the interaction among the constituents of the system, allowing one to control the volume of each “disk.”

With the previous assumptions  $H_{1b}$  becomes

$$H_{1b} = E_{kin} + V_{ext},$$

where

$$E_{kin} = -\frac{\hbar^2 \nabla^2}{2m},$$

$$V_{ext} = \frac{m}{2}(\Omega_x^2 x^2 + \Omega_\perp^2 \rho^2) + \frac{m\omega^2}{2K^2} \sin^2(Kx) \quad (3)$$

and the second term of  $V_{ext}$  represents the harmonic confinement of the magnetic trap, while the third one corresponds to the optical potential and  $\rho^2 = y^2 + z^2$ .

For future convenience, we write Eq. (3) as

$$H_{1b} = E_{kin} + \sum_j V_j + \left( V_{ext} - \sum_j V_j \right) \quad (4)$$

with

$$V_j = \Pi_j(x) \frac{m}{2} \left( \Omega_x^2 x_j^2 \frac{\pi^2}{k^2} + \omega^2 x_j^2 + \Omega_\perp^2 \rho^2 \right), \quad (5)$$

$\Pi_j(x) = \Pi(Kx/\pi - j)$ , where  $\Pi(x)$  is the rectangle function [ $\Pi(x) = 1$  for  $-1 \leq x < 1$ ,  $\Pi(x) = 0$  elsewhere],  $k = l_\perp K$  [with  $l_\perp = \sqrt{\hbar/(m\omega_\perp)}$ ], and  $x_j = (x - j\pi/k)$ . Here the harmonic axial confinement of the magnetic field has been considered as a site-dependent—with  $j$  the site index—constant additive term, merely shifting the local minima of the optical potential.

From Eq. (4) with the properties of the rectangle function we obtain

$$H_{1b} = \sum_j \Pi_j(x) [(E_{kin} + V_j) + (V_{ext} - V_j)]. \quad (6)$$

Hereafter the axial confinement of the magnetic trap will be neglected (small  $\Omega_x$ ).

We are now led to consider two different terms in Eq. (6). The first represents a local harmonic oscillator Hamiltonian

$$H_j^{ho} = \Pi_j(x) (E_{kin} + V_j) = \Pi_j(x) \left( \frac{\hbar^2 \nabla^2}{2m} + \frac{m\omega^2}{2} x_j^2 + \frac{m\Omega_\perp^2}{2} \rho^2 \right) \quad (7)$$

and a hopping one

$$H_j^{tunn} = \Pi_j(x) (V_{ext} - V_j) = \Pi_j(x) \left( \frac{m\omega^2}{2K^2} \sin^2(Kx) - \frac{m\omega^2}{2} x_j^2 \right). \quad (8)$$

The term  $V_j$  is the local second-order expansion of the optical potential; thus Eq. (8) represents the discrepancy between a harmonic potential and the true optical potential, describing hopping of atoms between neighboring sites.

Neutrality of the atoms, ensuring a finite-range interaction allows us to introduce a pseudopotential approximation (see, e.g., [36])

$$U(\mathbf{r}) = \sum_j \Pi_j(x) \tilde{a}_s \delta(\mathbf{r}) \frac{\partial}{\partial \mathbf{r}} \cdot \mathbf{r}, \quad \tilde{a}_s := \frac{4\pi\hbar^2 a_s}{m}, \quad (9)$$

where  $\mathbf{r}$  is the interatomic distance and  $a_s$  the  $s$ -wave scattering length ( $a_s$  in our approximation is considered constant). The validity of this model is ensured by the low energies involved in these interactions, a direct consequence of both the low-temperature limit (virtually zero) and the diluteness (low Fermi energy). In addition, the form of Eq. (9) shows that on-site terms only will contribute to the interaction Hamiltonian. Thus Eq. (1) can be rewritten in the form

$$\hat{H} = \sum_j \left( \int d\mathbf{r} \hat{\Psi}^\dagger(\mathbf{r}) [H_j^{ho}(\mathbf{r}) + H_j^{tunn}(\mathbf{r})] \hat{\Psi}(\mathbf{r}) + \tilde{a}_s \int d\mathbf{r} d\mathbf{r}' \hat{\Psi}^\dagger(\mathbf{r}) \hat{\Psi}^\dagger(\mathbf{r}') \delta(\mathbf{r} - \mathbf{r}') \hat{\Psi}(\mathbf{r}') \hat{\Psi}(\mathbf{r}) \right). \quad (10)$$

## B. The (space+local)-mode expansion

The choice of the basis for the expansion of the field operators is crucial. As already suggested by the grouping of terms in Eq. (7), we will choose a basis constituted by local harmonic oscillator eigenfunctions. In addition, because of the symmetry of the system we have chosen central-symmetric 2D harmonic oscillator (ho) eigenfunctions for the 2D isotropic radial ho [37]; instead of decomposing it in 1D ho eigenfunctions, this will give us deeper insight into conservation laws and selection rules imposed by the symmetries of the system. We then have

$$\hat{\Psi}(\mathbf{x}) = \sum_{i,n_x,J,m,\sigma} u_{n_x}(x - x_i) \mathcal{L}_{J,m}(\rho, \phi) \xi(\sigma) \hat{c}_{n_x, J, m, i, \sigma} \quad (11)$$

with

$$u_n(x) = \frac{1}{\sqrt{2^n n!} \sqrt{\pi} l_x} H_n(x/l_x) e^{-x^2/2l_x^2}, \quad (12)$$

$$\mathcal{L}_{J,m}(\rho, \phi) = \frac{e^{2im\phi}}{\sqrt{\pi} l_\perp} C_{Jm} \left( \frac{\rho}{l_\perp} \right)^{2m} L_{J-m}^{2J}(\rho/l_\perp), \quad (13)$$

$C_{Jm} = \sqrt{(J+m)!/(J-m)!}$ ,  $\xi(\sigma)$  a spin function, and  $l_x = \sqrt{\hbar/(m\omega_x)}$ .

In this decomposition  $u_n(x)$  is a 1D harmonic oscillator eigenfunction ( $H_n$  represents the  $n$ th Hermite polynomial) and  $\mathcal{L}_{J,m}$  a 2D harmonic oscillator eigenfunction [37] with  $L_{J-m}^J(x)$  a generalized Laguerre polynomial.

Fermionic operators will thus have five indices: three of them  $(n_x, J, m)$  identify (2+1)D local harmonic oscillator states, while  $i$  identifies the site and  $\sigma$  the spin. While  $n_x$  has its usual interpretation of the 1D harmonic oscillator number operator eigenvalue,  $J$  and  $m$  can be construed as angular momentum and  $x$ -axis component of the angular momentum, respectively.

This decomposition can be thought of as a generalized space-mode approximation, with additional local modes that, in the present case, correspond to the local (2+1)D harmonic oscillator quantum numbers. If not explicitly required, we will use  $\phi_\alpha = u_{n_\alpha}(x-x_{i_\alpha})\mathcal{L}_{J_\alpha, m_\alpha}(\rho, \phi)\xi(\sigma_\alpha)$ , with  $\alpha = \{n_\alpha, J_\alpha, m_\alpha, i_\alpha, \sigma_\alpha\}$  to simplify the index notation. We wish to stress that decomposition (11) is an *approximation* of the field  $\hat{\Psi}(\mathbf{x})$ : there is a non-nil overlapping between wave functions belonging to different sites, and thus orthogonality is not satisfied. Nevertheless, these overlapping integrals are supposed to be small, thus ensuring the consistency of this choice [10].

In the forthcoming calculation of the interaction term, Eq. (12) allows us to easily recognize that  $m$  is a conserved quantity. If we come back to Eq. (1) with the decomposition (11) we obtain

$$\begin{aligned} \hat{H} = & \sum_j \sum_{\alpha, \beta} \left( \int d\mathbf{r} \phi_\alpha^*(\mathbf{r}) H_j^{ho} \phi_\beta(\mathbf{r}) \hat{c}_\alpha^\dagger \hat{c}_\beta \right. \\ & + \int d\mathbf{r} \phi_\alpha^*(\mathbf{r}) H_j^{tunn} \phi_\beta(\mathbf{r}) \hat{c}_\alpha^\dagger \hat{c}_\beta \\ & + \tilde{a}_s \sum_{\gamma, \delta} \int d\mathbf{r} d\mathbf{r}' \phi_\alpha^*(\mathbf{r}) \phi_\gamma^*(\mathbf{r}') \delta(\mathbf{r} \\ & \left. - \mathbf{r}') \phi_\beta(\mathbf{r}) \phi_\delta(\mathbf{r}') \hat{c}_\alpha^\dagger \hat{c}_\beta^\dagger \hat{c}_\gamma \hat{c}_\delta \right). \end{aligned} \quad (14)$$

### III. HAMILTONIAN COEFFICIENTS

We are now in the position to calculate all the coefficients in Hamiltonian (14). The first term becomes

$$\hat{H}^{ho} = \sum_{j, \alpha, \beta} \lambda_\beta \int_{-\infty}^{\infty} d\mathbf{r} \Pi_j(x) \phi_\alpha^*(\mathbf{r}) \phi_\beta(\mathbf{r}) \hat{c}_\alpha^\dagger \hat{c}_\beta, \quad (15)$$

where  $\lambda_\beta$  is the (2+1)D harmonic oscillator eigenvalue

$$\lambda_{n_\beta J_\beta m_\beta i_\beta \sigma_\beta} = \left[ \hbar \omega_x \left( n_\beta + \frac{1}{2} \right) + \hbar (2J_\beta + 1) \right]. \quad (16)$$

Equation (15) can be written as

$$\sum_{j, \alpha, \beta} \lambda_\beta \delta_{\alpha, \beta} \delta_{i_\alpha j} \hat{c}_\alpha^\dagger \hat{c}_\beta = \sum_\alpha \lambda_\alpha \hat{n}_\alpha, \quad (17)$$

where the second Kronecker  $\delta$  is a consequence of the space-mode approximation, i.e., we consider only superpositions of

wave functions among which at least one is a local harmonic oscillator eigenfunction, while the first one stems from the orthogonality of the  $\phi_\gamma(x)$  functions.

We move now to the evaluation of the integral in the second term of Eq. (14), namely,

$$\hat{H}^{tunn} = \sum_{j, \alpha, \beta} \int d\mathbf{r} \phi_\alpha^*(\mathbf{r}) \Pi_j(x) H_j^{tunn}(x) \phi_\beta(\mathbf{r}) \quad (18)$$

where  $H_j^{tunn}(x)$  is independent of radial and spin degrees of freedom; we can rewrite Eq. (18) as

$$\begin{aligned} \hat{H}^{tunn} = & \sum_{j, \alpha, \beta} \delta_{J_\alpha J_\beta} \delta_{m_\alpha m_\beta} \delta_{\sigma_\alpha \sigma_\beta} \delta_{i_\alpha i_\beta} \\ & \times \int dx u_{n_\alpha}^*(x) H_j^{tunn}(x) u_{n_\beta}(x) \hat{c}_\alpha^\dagger \hat{c}_\beta. \end{aligned} \quad (19)$$

With the same assumptions of the local harmonic oscillator case the integral in Eq. (19) becomes

$$K_{n_\alpha n_\beta} \hbar \omega_x \int dy e^{-(y-\tau)^2/2} H_{n_\alpha}(y-\tau) H_j^{tunn}(y) e^{-y^2/2} H_{n_\beta}(y), \quad (20)$$

where  $K_{n_\alpha n_\beta} = (2^{n_\alpha + n_\beta} n_\alpha! n_\beta! \pi)^{-1/2}$  and we have put  $y = (x - i_\beta d) / l_x$  (where  $d = \pi/k$ ),  $\tau = (i_\beta - i_\alpha)$ , and  $\Omega = Kl_x$ . By substituting the expression of  $H_j^{tunn}(y)$  from Eq. (8) we obtain

$$\begin{aligned} K_{n_\alpha n_\beta} \hbar \omega_x \int dy e^{-[(y-\tau)^2 + y^2]/2} H_{n_\alpha}(y-\tau) H_{n_\beta}(y) \\ \times \left( \frac{1 - \cos(2\Omega y)}{4\Omega^2} - \frac{y^2}{2} \right) \hat{c}_\alpha^\dagger \hat{c}_\beta. \end{aligned} \quad (21)$$

If we define

$$\begin{aligned} T_{\alpha, \beta} = & \frac{K_{n_\alpha n_\beta}}{2} \delta_{J_\alpha J_\beta} \delta_{m_\alpha m_\beta} \delta_{\sigma_\alpha \sigma_\beta} \hbar \omega_x \int dy e^{-[(y-\tau)^2 + y^2]/2} \\ & \times H_{n_\beta}(y) H_{n_\alpha}(y-\tau) \left( \frac{y^2}{2} - \frac{1 - \cos(2\Omega y)}{4\Omega^2} \right), \end{aligned} \quad (22)$$

Eq. (19) becomes

$$\hat{H}^{tunn} = - \sum_{\alpha, \beta} T_{\alpha, \beta} \hat{c}_\alpha^\dagger \hat{c}_\beta. \quad (23)$$

Then the term  $T_{\alpha, \alpha} \hat{c}_\alpha^\dagger \hat{c}_\alpha$  can be incorporated into the  $\hat{H}^{ho}$  term, giving

$$\mu_\alpha = \lambda_\alpha - T_{\alpha, \alpha}. \quad (24)$$

We will here skip the explicit solution of the integral in Eq. (22), along with the analytic expression of  $T$ , which can be found in Appendix A. These calculations allow us to write

$$T_{\alpha, \beta} = \delta_{J_\alpha J_\beta} \delta_{m_\alpha m_\beta} \delta_{\sigma_\alpha \sigma_\beta} T_{n_\alpha n_\beta i_\alpha i_\beta}. \quad (25)$$

In Fig. 2 we have plotted the coefficient  $T_{n_\alpha n_\beta i_\alpha i_\beta}$  as a function of the ratio between distance and the period of the optical lattice, for  $n_\alpha, n_\beta = 0, 1$ . The points corresponding to

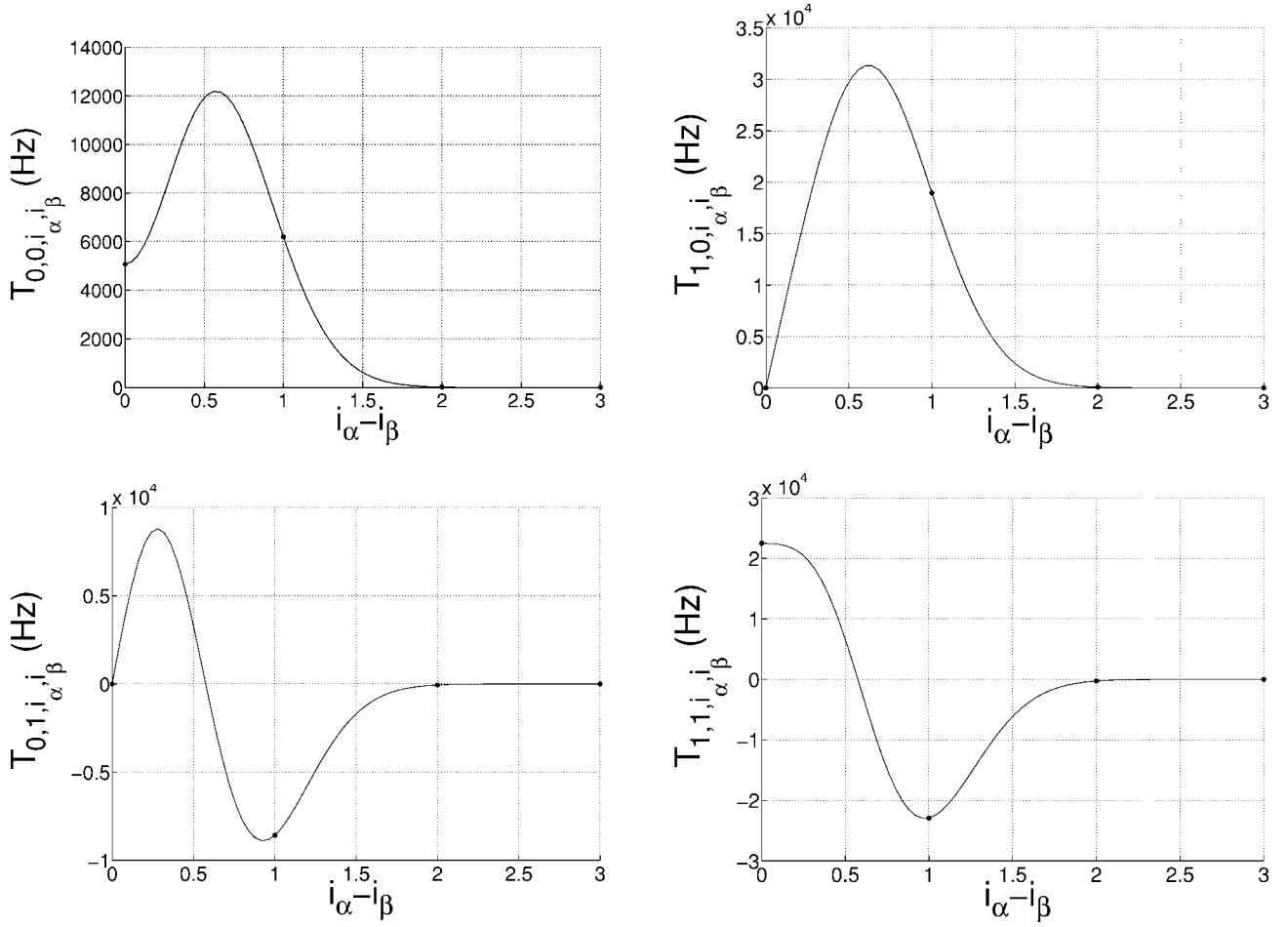


FIG. 2. Plots of the tunneling coefficients from  $T_{00}$  to  $T_{11}$ . A detailed discussion of the analytic expression of the hopping parameter will be given in Appendix A. See also Fig. 8 below.

discrete values of the ratio  $x/d$ , i.e., the points with a relevant physical meaning have been marked in each plot. The values of  $T$  plotted throughout the paper are in angular frequency units (e.g.,  $\omega = E/\hbar$ ); moreover  $\theta = \pi$  and  $s = 1$  unless otherwise specified. Even if the correctness of the above procedure seems undoubted, it must be remembered that it is entirely based on the space-mode approximation, whose validity depends on the overlapping of wave functions belonging to different sites and thus might be violated.

These plots show how the tunneling amplitude varies with the distance. In particular it is clear how, for long-distance tunneling, there is a negative exponential dependence. Nevertheless, if the experimental conditions are properly chosen (i.e., angle between counterpropagating laser beams and their power), it is possible to obtain conditions where, for instance, nearest-neighbor and next-to-nearest-neighbor tunneling coefficients have opposite signs (see, e.g., Fig. 3,  $T_{0,0,i_{\alpha},i_{\beta}}$ ), and thus the model, in that case, might exhibit frustration.

We will now move to the determination of the interaction term, namely, the last term of Eq. (14). As a first step, we can write the integral in cylindrical coordinates,

$$\begin{aligned}
 \tilde{a}_s & \int d\mathbf{r} d\mathbf{r}' \phi_{\alpha}^*(\mathbf{r}) \phi_{\gamma}^*(\mathbf{r}') \delta(\mathbf{r} - \mathbf{r}') \phi_{\beta}(\mathbf{r}) \phi_{\delta}(\mathbf{r}') \\
 & = \tilde{a}_s \int dx dx' u_{n_{\alpha}}^*(x - x_{i_{\alpha}}) u_{n_{\gamma}}^*(x' - x_{i_{\gamma}}) \delta(x - x') u_{n_{\beta}}(x \\
 & \quad - x_{i_{\beta}}) u_{n_{\delta}}(x' - x_{i_{\delta}}) \\
 & \quad \times \int d\tilde{\rho} d\tilde{\rho}' \frac{\tilde{\rho}}{\pi} \int d\phi d\phi' \mathcal{L}_{J_{\alpha} m_{\alpha}}^*(\tilde{\rho}, \phi) \mathcal{L}_{J_{\gamma} m_{\gamma}}^*(\tilde{\rho}', \phi') \delta(\rho \\
 & \quad - \rho') \delta(\phi - \phi') \mathcal{L}_{J_{\beta} m_{\beta}}(\tilde{\rho}, \phi) \mathcal{L}_{J_{\delta} m_{\delta}}(\tilde{\rho}', \phi') \quad (26)
 \end{aligned}$$

with  $\tilde{\rho} = \rho/l_{\rho}$  and the identity

$$\delta(\mathbf{r}) = \frac{\delta(\rho)\delta(\phi)}{\pi\rho}.$$

As we are dealing with a short-range interaction modeled by a  $\delta(\mathbf{r} - \mathbf{r}')$  function, we will consider on-site interaction only ( $\tilde{x}_{i_{\alpha}} = \tilde{x}_{i_{\beta}} = \tilde{x}_{i_{\delta}} = \tilde{x}_{i_{\gamma}}$ ).

This choice is completely justified because the interaction term is modeled by a pseudopotential term for which nearest-neighbor interactions become negligible. In this case the first

integral on the left-hand side of Eq. (26) reduces to

$$U_x = \frac{1}{\pi l_x} \sqrt{\frac{2^{-(n_\alpha+n_\beta+n_\gamma+n_\delta)}}{n_\alpha! n_\beta! n_\gamma! n_\delta!}} \times \int d\tilde{x} H_{n_\alpha}(\tilde{x}) H_{n_\beta}(\tilde{x}) H_{n_\gamma}(\tilde{x}) H_{n_\delta}(\tilde{x}) e^{-2\tilde{x}^2} \quad (27)$$

with  $\tilde{x}=x/l_x$ , whose explicit calculation is given in Appendix B. Here we just give the final result,

$$U_x = \frac{\delta_{\|\bar{n}\|,2N}}{\pi l_x} \sum_{\bar{s}}^{\bar{n}} \frac{\Xi(\bar{s})}{\sqrt{2}^{\|\bar{s}\|+3}} \Gamma\left(\frac{(\|\bar{n}\| - \|\bar{s}\|)}{2} + 1\right) \quad (28)$$

with

$$\Xi(\bar{s}) = \begin{cases} 0 & \text{if } s_\theta \text{ odd,} \\ \prod_{\theta} \frac{1}{n_\theta!} \binom{n_\theta}{s_\theta} H_{s_\theta}(0) & \text{if } s_\theta \text{ even.} \end{cases} \quad (29)$$

The summation is to be intended as four separate summations over the components of a vector  $\bar{s}=\{s_\alpha, s_\beta, s_\gamma, s_\delta\}$  from  $\{0, 0, 0, 0\}$  to  $\bar{n}=\{n_\alpha, n_\beta, n_\gamma, n_\delta\}$ . The norm  $\|\bar{x}\|$  is a one-norm ( $\|\bar{x}\|=\sum_\theta |x_\theta|$ ,  $\theta=\alpha, \beta, \gamma, \delta$ ) and the  $\delta$  in Eq. (27) represents the parity selection rule, obtained from the explicit calculation of the integral.

The radial part of the integral can be explicitly written as

$$U_\rho = \int \int d\rho d\phi \frac{\rho}{\pi} \mathcal{L}_{J_\alpha m_\alpha}^*(\rho, \phi) \mathcal{L}_{J_\gamma m_\gamma}^*(\rho, \phi) \mathcal{L}_{J_\beta m_\beta}(\rho, \phi) \times \mathcal{L}_{J_\delta m_\delta}(\rho, \phi). \quad (30)$$

With the definition given by Eq. (12), we can easily perform the angular integration and we obtain

$$U_\rho = \frac{2\delta_{m_\alpha+m_\gamma, m_\beta+m_\delta}}{\pi^2} \int_0^\infty d\rho \rho R_{J_\alpha m_\alpha}^*(\rho) R_{J_\gamma m_\gamma}^*(\rho) \times R_{J_\beta m_\beta}(\rho) R_{J_\delta m_\delta}(\rho). \quad (31)$$

The reader is again addressed to Appendix B for the explicit evaluation of the integral in Eq. (31). The result is given by

$$U_\rho = \frac{\delta_{m_\alpha+m_\gamma, m_\beta+m_\delta}}{\pi^2 l_\perp^2} \sum_{\bar{q}=\|\bar{m}\|}^{\bar{J}} \Lambda(\bar{J}, \bar{m}, \bar{q}) \frac{\Gamma(\|\bar{q}\| + 3/2)}{2^{\|\bar{q}\|+3/2}} \quad (32)$$

with

$$\Lambda(\bar{J}, \bar{m}, \bar{q}) = \prod_{\theta=\alpha, \beta, \gamma, \delta} \frac{(-1)^{J_\theta - q_\theta} \sqrt{(J_\theta + m_\theta)! (J_\theta - m_\theta)!}}{(J_\theta - q_\theta)! (q_\theta + m_\theta)! (q_\theta - m_\theta)!} \quad (33)$$

and, following previous notation,  $\bar{q}=\{q_\alpha, q_\beta, q_\gamma, q_\delta\}$ ,  $\bar{J}=\{J_\alpha, J_\beta, J_\gamma, J_\delta\}$ , and  $\bar{m}=\{|m_\alpha|, |m_\beta|, |m_\gamma|, |m_\delta|\}$ . The overall interaction coefficient can then be written as the product of Eqs. (32) and (28),

$$U_{\alpha, \beta, \gamma, \delta} = \delta_{\|\bar{n}\|, 2N} \delta_{m_\alpha+m_\beta, m_\gamma+m_\delta} \frac{\bar{a}_s}{4l_x \pi^3 l_\perp^2} \sum_{\bar{q}=\|\bar{m}\|}^{\bar{J}} \sum_{\bar{s}}^{\bar{n}} \frac{\Lambda(\bar{J}, \bar{m}, \bar{q}) \Xi(\bar{s})}{\sqrt{2}^{\|\bar{s}\|+2\|\bar{q}\|}} \times \Gamma\left(\|\bar{q}\| + \frac{3}{2}\right) \Gamma\left(\frac{(\|\bar{n}\| - \|\bar{s}\| + 1)}{2}\right). \quad (34)$$

We are thus enabled to rewrite Hamiltonian (14) in terms of the calculated coefficients, obtaining

$$\hat{H} = \sum_j \left( \sum_\alpha \lambda_\alpha \hat{n}_\alpha^\dagger + \sum_{\alpha, \beta} T_{\alpha, \beta} \hat{c}_\alpha^\dagger \hat{c}_\beta + \sum_{\alpha, \beta, \gamma, \delta} U_{\alpha, \beta, \gamma, \delta} \hat{c}_\alpha^\dagger \hat{c}_\beta^\dagger \hat{c}_\gamma \hat{c}_\delta \right). \quad (35)$$

We will refer to Eq. (35) as the generalized Hubbard Hamiltonian. For sake of simplicity, in Eq. (35) we have not written down explicitly the selection rules imposed by symmetry constraints (see below).

### A. Symmetry properties of the interaction term

In addition to global symmetry properties, such as (1) rotational symmetry along the  $x$  axis and (2) left-right symmetry, reflected by momentum  $x$ -component conservation and parity conservation for the 1D harmonic oscillators along the  $x$  axis, it is clear from Eq. (34) that the coefficient  $U_{\alpha, \beta, \gamma, \delta}$  has some symmetry properties: (a)  $U$  does not depend on the sign of  $m_\chi$  with  $\chi=\alpha, \beta, \gamma, \delta$ , provided  $m$  is conserved during the interaction ( $m_\alpha+m_\beta=m_\gamma+m_\delta$ ); (b)  $U$  possesses a permutational symmetry, namely,

$$U_{\alpha, \beta, \gamma, \delta} = U_{\beta, \alpha, \gamma, \delta} = U_{\alpha, \beta, \delta, \gamma} = U_{\beta, \alpha, \delta, \gamma} \quad (36)$$

We would like to draw the reader's attention to the two  $\delta$  functions in Eq. (34) which make explicit the conservation laws that might have been expected by simply considering the symmetry of the problem. The first one represents parity conservation, and the second conservation of the  $x$  component of the angular momentum. In Table I, we give the analytical value of  $U$  for interaction between particles belonging to the first three shells of the 2D radial harmonic oscillator and to the first level for the axial harmonic oscillator. These symmetry constraints allow us to class the possible quantum numbers of the interacting particles according to the value of the corresponding  $U$ . For example, for

$$\alpha = \{0, 1, 0, i, \sigma\}, \quad \beta = \{0, 0, 0, i, \sigma'\},$$

$$\delta = \{0, 0, 0, i, \sigma\}, \quad \gamma = \{0, 0, 0, i, \sigma'\},$$

and

$$\alpha = \{0, 0, 0, i, \sigma\}, \quad \beta = \{0, 0, 0, i, \sigma'\},$$

$$\delta = \{0, 1, 0, i, \sigma\}, \quad \gamma = \{0, 0, 0, i, \sigma'\},$$

we have the same value of  $U$ , henceforth the class definition of Table I. We would like to point out two aspects of this example. First of all it may be noticed that the angular momentum  $J$  is not conserved throughout the interaction: this is a general feature of the system considered; there is no global rotational symmetry but only in the plane orthogonal to the

TABLE I. Values of  $\tilde{U}_{\alpha,\beta,\gamma,\delta}=[\hbar^2 a_s l(m l_x \pi^2 l_\perp^2)]^{-1} U_{\alpha,\beta,\gamma,\delta}$  for  $\{n_\alpha, n_\beta, n_\gamma, n_\delta\}=\{0, 0, 0, 0\}$ ,  $i_\alpha=i_\beta$ , and  $\sigma$  and  $\sigma'$  satisfy symmetry constraints. The value  $m_\chi$  represents the equivalence class described in the text.

$J_\alpha$	$J_\beta$	$J_\gamma$	$J_\delta$	$m_\alpha^*$	$m_\beta^*$	$m_\gamma^*$	$m_\delta^*$	$\tilde{U}_{\alpha,\beta,\gamma,\delta}$
0	0	0	0	0	0	0	0	$\pi/2^4$
1/2	1/2	1/2	1/2	1/2	1/2	1/2	1/2	$15\pi/2^8$
1	1	1	1	1	1	1	1	$945\pi/2^{14}$
1	1/2	1/2	1	1	1/2	1/2	1	$105\pi/2^{11}$
1	1	1	1	0	0	0	0	$193\pi/2^{12}$
1/2	0	1/2	0	1/2	0	1/2	0	$3\pi/2^6$
1	1	1	1	1	0	1	0	$345\pi/2^{13}$
1	1/2	1/2	1	0	1/2	1/2	0	$33\pi/2^{10}$
1	1/2	1/2	1	0	1/2	-1/2	1	$45\pi/2^{10}\sqrt{2}$
1	0	1	0	1	0	1	0	$15\pi/2^9$
1	1	0	0	0	0	0	0	$7\pi/2^8$
1	1	1	0	1	-1	0	0	$45\pi/2^{10}$
1	1/2	1/2	0	0	1/2	1/2	0	$3\pi/2^8$
1	0	0	0	0	0	0	0	$-\pi/2^6$

1D optical lattice. Moreover, in this particular interaction the value for the coefficient  $U$  is negative; this appears to be a rare (but not unique) situation. The implications of this condition will be pointed out in Sec. IV

#### IV. SPECIAL CASES

In this section we derive three model Hamiltonians for fermions in optical lattices. We consider, for all cases, only the lowest-state axial quantum number (i.e.,  $n_\alpha=n_\beta=0$ ). Hence  $T_{\alpha,\beta}$  can be written as

$$T_{\alpha,\beta} = \delta_{J_\alpha J_\beta} \delta_{m_\alpha m_\beta} \delta_{\sigma_\alpha \sigma_\beta} T_{0,0,i_\alpha i_\beta}. \quad (37)$$

As far as an ultracold gas is considered, it seems feasible to restrict our analysis to the first few levels above the ground state (i.e.,  $J_\alpha=0, 1/2, \dots$ ). This regime can be attained experimentally, considering a situation where  $\hbar\omega_x \gg \hbar\Omega_\perp > k_B T$ , and thus for a low number of atoms radial states only can be populated. As a first example, we consider the case having  $J_\alpha=0$  as the only radial level allowed. This approximation might be suitable for mean site occupation numbers  $N_i \leq 2$  and for  $\hbar\Omega_\perp \gg k_B T$ . Taking into account spin degeneracy, it seems feasible to assume that the dynamics is confined to the single-site ground-state energy levels, in strict analogy to what is done for a confined Bose gas [5]. From Eq. (34), along with the previous assumptions, we obtain [38]

$$\hat{H} = \sum_{i,\sigma} \mu_i \hat{n}_{i,\sigma} - T \sum_{i,\sigma} (\hat{c}_{i,\sigma}^\dagger \hat{c}_{i+1,\sigma} + \hat{c}_{i+1,\sigma}^\dagger \hat{c}_{i,\sigma}) + U \sum_{i,\sigma,\sigma'} \hat{n}_{i,\sigma} \hat{n}_{i,\sigma'} \quad (38)$$

with  $T=T_{0,0,i_\alpha i_\alpha+1}$  which is easily recognized as the Hubbard Hamiltonian, whose role in the ultracold-atom physics has been pointed out elsewhere [5,29]. Note that in this example we have made the assumption that the tunneling coefficient

is significantly different from zero only for nearest-neighboring sites. Nevertheless, more involved situations may arise, suggesting interesting physical features, as is shown in Appendix A (Fig. 8).

If we now consider a spin-polarized gas (for the experimental feasibility of this regime, see, e.g., [39]) in a (radial) multilevel system we obtain [38]

$$\hat{H} = \sum_{\bar{n},i} \mu_{\bar{n},i} \hat{n}_{\bar{n},i} - T \sum_{\bar{n},i} (\hat{c}_{\bar{n},i}^\dagger \hat{c}_{\bar{n},i+1} + \hat{c}_{\bar{n},i+1}^\dagger \hat{c}_{\bar{n},i}), \quad (39)$$

where  $\bar{n}=(n_\alpha, J_\alpha, m_\alpha, \sigma_\alpha)$ , and the absence of the interaction term is related to the symmetry properties of the coefficient  $U_{\alpha\beta\gamma\delta}$ . We would like to point out that, in this case, the particle number limit is given only by the prescription  $n_\alpha=0$ .

The Hamiltonian (39) is readily diagonalized to yield

$$\hat{H} = \sum_{\bar{n}} \hat{H}_{\bar{n}} = \sum_{\bar{n},k,\sigma} [\mu_{\bar{n}} - 2T \cos(k)] \hat{n}_{\bar{n},k,\sigma} \quad (40)$$

with the same procedure followed in the strong-coupling limit in the Hubbard Hamiltonian.

#### A. Rotational Hubbard Hamiltonian

As a last example, we derive a third Hamiltonian that may give the reader some insight into the increasing complexity if higher single-particle levels are taken into account. Here we consider a situation where we allow  $J_\alpha=0, 1/2$ , partly relaxing then the conditions on particle numbers and temperature that led us to the Hubbard model. Even in this situation we keep  $n_\alpha=0$ , and thus  $T_{n_\alpha i_\alpha n_\beta i_\alpha+1}=T$  as already pointed out:

$$H_{2 \text{ level}} = \sum_{i,\sigma} \sum_{a=-1}^1 [\mu_a n_{i,a,\sigma} - T(c_{i,a,\sigma}^\dagger c_{i+1,a,\sigma} + c_{i+1,a,\sigma}^\dagger c_{i,a,\sigma})] \\ + \sum_i \sum_{a,b,c,d} U_{a,b,c,d} \sum_{\sigma,\sigma'} c_{i,a,\sigma}^\dagger c_{i,b,\sigma'}^\dagger c_{i,d,\sigma'} c_{i,c,\sigma}, \quad (41)$$

where  $U_{a,b,c,d} = U_{a,i_\alpha; b,i_\beta; c,i_\gamma; d,i_\delta}$ . The label  $a$  (as well as  $b$ ,  $c$ , and  $d$ ) has been introduced to represent the triplet of harmonic oscillator numbers  $(n_\alpha, J_\alpha, m_\alpha)$ ; hence  $\alpha = \{a, i_\alpha, \sigma_a\}$ . One should recall that originally  $\alpha = (n_\alpha, J_\alpha, m_\alpha, i_\alpha, \sigma_a)$ . Here, however, it is convenient to write in an explicit way both spin indices  $\sigma_\alpha$  and site indices  $i_\alpha$ .

The triplet  $a = (n_\alpha, J_\alpha, m_\alpha)$  is such that the value  $a=0$  corresponds to  $(0, 0, 0)$ ,  $a=1 \rightarrow (0, 1/2, +1/2)$ , and  $a=-1 \rightarrow (0, 1/2, -1/2)$ . The axial quantum number  $n_x$  has been “frozen” to 0 due to the disk-shaped potential form (i.e.,  $\omega_x \gg \omega_\perp$ ) while the radial quantum number  $J$  has been limited to the values  $\{0, 1/2\}$  as a first approximation beyond  $J=0$  [Hubbard Hamiltonian, see Eq. (38)]. The present model thus enriches the dynamical scenario by introducing modes that takes into account the simplest possible rotational processes for fermions confined in a well, describing situations with higher number of fermions per site.

The wealth of the scenario depicted in Eq. (41) arises from the level dependence of the interaction coefficient  $U_{a,b,c,d}$ . In fact  $U_{a,b,c,d}$ , as a function of the energy levels may provide a useful tool to simplify Eq. (41) hinting at the best strategy for both numerical and analytical analysis of this model. Two main aspects concerning these coefficients are worth repeating here: (a) the  $m_\alpha$ -conserving nature of the interaction, related to the symmetry properties of the confining potential and of the interaction coefficient (see Sec. III A), reduces the number of possible processes; (b) the symmetry properties of  $U_{\alpha,\beta,\gamma,\delta}$  [see Eq. (36)] allow the grouping of interaction terms, according to what has been done in Table I.

From a general point of view, in Hamiltonian (41) the hopping factor may be construed as a multichannel tunneling coefficient, where the radial quantum numbers identify the channel label, in the same spirit of Hamiltonian (40). Incidentally, this is true if axial degrees of freedom are frozen to  $n_\alpha = n_\beta = 0$ ; otherwise there is tunneling among levels with  $n_\alpha \neq n_\beta$ , for some  $\alpha$  and  $\beta$ .

Hamiltonian (41) can represent a situation where single traps are loaded with a small number of atoms, so as to fill the first two radial levels of the local harmonic oscillator. To experimentally obtain one of the different simplified Hamiltonians—like (41)—it is necessary to have control of four experimental parameters: laser intensity, angle between counterpropagating lasers, axial magnetic trapping frequency, scattering length. With these parameters it is possible to gain full knowledge of the “lattice constant,” interaction parameter, shape, and depth of the 3D harmonic traps. The most critical point seems the few-atom loading of the trap but a technique involving a 3D anisotropic array—a sort of 2D array of 1D arrays—might overcome the problem.

In this picture, the interaction coefficient  $U$  can then be used as a source of entanglement between different channels. Moreover, the possibility of experimental control of the scattering length, and thus of the interaction term, via an applied magnetic field may provide a useful tool of external manipulation of the state of the system in the rich scenario here depicted.

To outline future paths of research, we will here sketch a way to set up a mean-field procedure for the rotational Hubbard Hamiltonian (RHH). The main interest of this approach resides in the possibility of a general discussion of some features of the model which have a direct experimental relevance. For example, it is possible to state that, according to what is usually affirmed in the literature [33], no BCS-like ground state is possible for repulsive interaction, while for an attractive two-body potential a paired ground state is possible. The flexibility of experimental techniques involved in the study of ultracold-atom physics allows us to envisage experimental conditions where these two different regimes are attained. For example, exploiting a Feshbach resonance it is possible to drive the scattering length  $a_s$  from positive to negative values, leading thus the system through a quantum phase transition.

The analytic procedure adopted hereafter deeply relies on the concept of a quasifree state [33]. In our situation the following definition of a quasifree state can be adopted: (I) all correlation functions can be computed from Wick’s theorem; (II) four-fermionic expectation values over the quasifree state have the form

$$\langle \phi | e_1 e_2 e_3 e_4 | \phi \rangle = \langle \phi | e_1 e_2 | \phi \rangle \langle \phi | e_3 e_4 | \phi \rangle - \langle \phi | e_1 e_3 | \phi \rangle \\ \times \langle \phi | e_2 e_4 | \phi \rangle + \langle \phi | e_1 e_4 | \phi \rangle \langle \phi | e_2 e_3 | \phi \rangle$$

with  $e_i = c_i, c_i^\dagger$ . In particular we would like to point out how the three terms on the right-hand side will lead to the direct, the exchange, and the pairing energy terms of a Hartree-Fock-Bogoliubov mean-field Hamiltonian, which, for our RHH becomes

$$\hat{H}_{2 \text{ level}}^{HFB} = \hat{H}_0 + \sum_{\substack{i,a,b,c,d, \\ \sigma \neq \sigma'}} U_{a,b,c,d} (\chi_{i,a,\sigma,d,\sigma} \hat{c}_{i,b,\sigma'}^\dagger \hat{c}_{i,c,\sigma'} \\ + \chi_{i,c,\sigma',b,\sigma'} \hat{c}_{i,a,\sigma}^\dagger \hat{c}_{i,d,\sigma} - \chi_{i,d,\sigma,b,\sigma'} \hat{c}_{i,a,\sigma}^\dagger \hat{c}_{i,c,\sigma'} \\ - \chi_{i,c,\sigma',a,\sigma} \hat{c}_{i,b,\sigma'}^\dagger \hat{c}_{i,d,\sigma} + \xi_{i,b,\sigma',a,\sigma}^* \hat{c}_{i,c,\sigma'} \hat{c}_{i,d,\sigma} \\ + \xi_{i,d,\sigma,c,\sigma'} \hat{c}_{i,a,\sigma}^\dagger \hat{c}_{i,b,\sigma'}^\dagger)$$

with

$$\hat{H}_0 = \sum_{i,a,\sigma} [\lambda_a \hat{n}_{i,a,\sigma} + T(\hat{c}_{i+1,a,\sigma}^\dagger \hat{c}_{i,a,\sigma} + \text{H.c.})],$$

$$\chi_{i,a,\sigma,b,\sigma'} = \langle \phi_{HFB} | \hat{c}_{i,a,\sigma}^\dagger \hat{c}_{i,b,\sigma'} | \phi_{HFB} \rangle,$$

$$\xi_{i,a,\sigma,b,\sigma'} = \langle \phi_{HFB} | \hat{c}_{i,a,\sigma} \hat{c}_{i,b,\sigma'} | \phi_{HFB} \rangle.$$

The set of generators  $\{\hat{c}_\alpha^\dagger \hat{c}_\beta - \frac{1}{2} \delta_{\alpha\beta} (1 \leq \alpha \neq \beta \leq r), \hat{c}_\alpha \hat{c}_\beta, \hat{c}_\alpha^\dagger \hat{c}_\beta^\dagger (1 \leq \alpha \neq \beta \leq r)\}$  obeys the following commutation relations:



$$\left[ \hat{c}_i^\dagger \hat{c}_j - \frac{1}{2} \delta_{ij} \hat{c}_k^\dagger \hat{c}_l - \frac{1}{2} \delta_{kl} \right] = \delta_{jk} \left( \hat{c}_i^\dagger \hat{c}_l - \frac{1}{2} \delta_{il} \right),$$

$$\left[ \hat{c}_i^\dagger \hat{c}_j - \frac{1}{2} \delta_{ij} \hat{c}_k^\dagger \hat{c}_l \right] = \delta_{jk} \hat{c}_i^\dagger \hat{c}_l - \delta_{jl} \hat{c}_i^\dagger \hat{c}_k,$$

$$\begin{aligned} [\hat{c}_i \hat{c}_j, \hat{c}_k^\dagger \hat{c}_l^\dagger] &= \delta_{ik} \left( \hat{c}_l^\dagger \hat{c}_j - \frac{1}{2} \delta_{lj} \right) + \delta_{lj} (\hat{c}_k^\dagger \hat{c}_i - 1/2 \delta_{ki}) - \delta_{li} (\hat{c}_k^\dagger \hat{c}_j \\ &\quad - 1/2 \delta_{kj}) - \delta_{kj} (\hat{c}_l^\dagger \hat{c}_i - 1/2 \delta_{li}), \end{aligned} \quad (42)$$

allowing us to state that the dynamical algebra of this new Hamiltonian, which is now quadratic in terms of  $\hat{c}_i$ ,  $\hat{c}_i^\dagger$ , can be easily recognized to be  $so(2r)$  [34] (where  $r$  is the number of single-particle states).

Having determined the dynamical algebra of the model Hamiltonian, this enables us—at least in principle—to find the ground state of the system with a straightforward procedure. As will be clear from the subsequent discussion, the main difficulties arise as the number of generators of the  $so(2r)$  algebra grows with  $r(2r-1)$ . For instance for the two-site,  $J=0, 1/2$  model (i.e.,  $r=12$ ), the Hamiltonian dynamical algebra will have 276 generators.

In spite of the technical difficulties (both analytical and numerical), it is appropriate to apply algebraic techniques to diagonalize  $\hat{H}_{2\text{-level}}^{HFB}$ . As stated before, this general approach will give some insight into the ground-state properties of the system. If we consider a unitary transformation  $g \in SO(2r)$  we can write

$$\hat{H}_d = g \hat{H}_{2\text{-level}}^{HFB} g^{-1}, \quad (43)$$

where  $\hat{H}_d$  is diagonal. As a direct consequence the ground state  $|\phi_{HFB}\rangle$  of  $\hat{H}_{2\text{-level}}^{HFB}$  can be written as

$$|\phi_{HFB}\rangle = g|0,0,0,\dots,0,0\rangle = g|0\rangle, \quad (44)$$

where  $|0\rangle$  can be defined as the Bogoliubov particle vacuum (ground state of  $\hat{H}_d$ ). Following [34],  $|0\rangle$  represents a possible choice for the extremal state for the  $SO(2r)$  group with

$U(r)$  as the corresponding maximum stability subgroup [ $h \in U(r)$ ]. This entails

$$g|0\rangle = \Omega h|0\rangle = \Omega|0\rangle e^{i\phi(h)}, \quad (45)$$

where

$$\Omega = \exp \sum_{1 \leq \alpha \neq \beta \leq r} (\eta_{\alpha,\beta} \hat{c}_\alpha^\dagger \hat{c}_\beta^\dagger - \text{H.c.}) \in \frac{SO(2r)}{U(r)}. \quad (46)$$

The phase appearing in Eq. (45) has no relevance for our purposes, as we are interested in the evaluation of observable expectation values.

The problem mentioned above about the size of the dynamical algebra appears here with all its implications. It is necessary to exponentiate the operator  $\sum_{1 \leq \alpha \neq \beta \leq r} (\eta_{\alpha,\beta} \hat{c}_\alpha^\dagger \hat{c}_\beta^\dagger - \text{H.c.})$  which is a  $2r \times 2r$  matrix in the faithful matrix representation.

Nevertheless, for a repulsive two-body potential, the pairing term can be neglected [33]; thus the dynamical algebra of the system becomes  $U(r)$ . Following [34], we can express the Hamiltonian ground state as

$$|\phi_{HFB}\rangle = \exp \sum_{\substack{k+1 \leq \alpha \leq r \\ 1 \leq j \leq k}} (\eta_{\alpha,\beta} \hat{c}_\alpha^\dagger \hat{c}_\beta - \text{H.c.}) |0\rangle, \quad (47)$$

where

$$|0\rangle = |0, \dots, 0\rangle, \quad (48)$$

which is, in fact, the ground state of the noninteracting Hamiltonian. It is worth noticing that this general procedure can be greatly simplified if further constraints, related to symmetries of the problem, are imposed onto the coefficients  $\eta_{\alpha,\beta}$ . For example, if we consider the two-site ( $A,B$ ),  $J=0, 1/2$  case, due to Eq. (37) the matrix  $\bar{\eta}$  with elements  $\eta_{\alpha,\beta}$  will have the form

$$\bar{\eta} = \begin{pmatrix} 0 & \eta_{1,2} & \eta_{1,3} & \eta_{1,4} & \eta_{1,5} & \eta_{1,6} & \eta_{1,7} & 0 & 0 & 0 & 0 & 0 \\ -\eta_{1,2} & 0 & \eta_{2,3} & \eta_{2,4} & \eta_{2,5} & \eta_{2,6} & 0 & \eta_{2,8} & 0 & 0 & 0 & 0 \\ -\eta_{1,3} & -\eta_{2,3} & 0 & \eta_{3,4} & \eta_{3,5} & \eta_{3,6} & 0 & 0 & \eta_{3,9} & 0 & 0 & 0 \\ -\eta_{1,4} & -\eta_{2,4} & -\eta_{3,4} & 0 & \eta_{4,5} & \eta_{4,6} & 0 & 0 & 0 & \eta_{4,10} & 0 & 0 \\ -\eta_{1,5} & -\eta_{2,5} & -\eta_{3,5} & -\eta_{4,5} & 0 & \eta_{5,6} & 0 & 0 & 0 & 0 & \eta_{5,11} & 0 \\ -\eta_{1,6} & -\eta_{2,6} & -\eta_{3,6} & -\eta_{4,6} & -\eta_{5,6} & 0 & 0 & 0 & 0 & 0 & 0 & \eta_{6,12} \\ -\eta_{1,7} & 0 & 0 & 0 & 0 & 0 & 0 & 0 & 0 & 0 & 0 & 0 \\ 0 & -\eta_{2,8} & 0 & 0 & 0 & 0 & 0 & 0 & 0 & 0 & 0 & 0 \\ 0 & 0 & -\eta_{3,9} & 0 & 0 & 0 & 0 & 0 & 0 & 0 & 0 & 0 \\ 0 & 0 & 0 & -\eta_{4,10} & 0 & 0 & 0 & 0 & 0 & 0 & 0 & 0 \\ 0 & 0 & 0 & 0 & -\eta_{5,11} & 0 & 0 & 0 & 0 & 0 & 0 & 0 \\ 0 & 0 & 0 & 0 & 0 & -\eta_{6,12} & 0 & 0 & 0 & 0 & 0 & 0 \end{pmatrix}, \quad (49)$$

thus impressively reducing the computational effort needed to evaluate the exponential in Eq. (46). In Eq. (49) we have assumed the following convention:

$$\begin{aligned} \{n_\alpha=0, J_\alpha=0, m_\alpha=0, i_\alpha=A, \sigma_\alpha=\uparrow\} &\rightarrow 1, \\ \{n_\alpha=0, J_\alpha=0, m_\alpha=0, i_\alpha=A, \sigma_\alpha=\downarrow\} &\rightarrow 2, \\ &\vdots \\ \{n_\alpha=0, J_\alpha=0, m_\alpha=0, i_\alpha=B, \sigma_\alpha=\uparrow\} &\rightarrow 7, \\ \{n_\alpha=0, J_\alpha=0, m_\alpha=0, i_\alpha=B, \sigma_\alpha=\downarrow\} &\rightarrow 8, \\ &\vdots \end{aligned}$$

### V. CONCLUSIONS

In this paper we have investigated the complex structure of fermion interactions for a fermion gas distributed in a linear periodic array of potential wells. Based on the standard many-fermion quantum field theory endowed with a potential distribution mimicking a realistic experimental setup, we have calculated analytically the hopping and interaction coefficients that describe the interactions of fermions within a generalized multimode Hubbard Hamiltonian. Their dependence on the external adjustable parameters (such as laser intensity, magnetic trap frequency, wavelength, and scattering length) has been determined.

Our analysis shows that, except for two particularly simple cases (the gas of spin-unpolarized fermions and the gas of noninteracting spin-polarized fermions), models with different degrees of complexity can be derived depending on the interaction processes one decides to account for or to neglect [consider, e.g., that, in principle, one might introduce an unlimited number of (local) rotational levels]. In this respect, our simplest nontrivial model (41), which is able to account for the (local) rotational activity of fermions, appears to be far more complex than the Hubbard model or the spin-polarized noninteracting model derived in Sec. IV.

Therefore, the first objective of our future work is to perform a systematic study of model (41). Based on the present analysis and exploiting the interaction-parameter scenario here depicted, the second objective is to recognize the significant regimes characterizing the confined fermion gas and to derive the relevant models from Eq. (35).

We would like to stress once again how the analytical knowledge of the coefficients in principle allows us to tailor Hamiltonians performing specific tasks.

An aspect that certainly deserves attention is the study of the zero-temperature phase diagram of model (41) (and, more in general, of sufficiently simple—and thus tractable—models derived from the GHH) and of the relevant phenomenology aimed at suggesting new possible experiments. To achieve a reliable description of these systems, several established analytical and numerical approaches (see, e.g., [40–44], respectively) can be implemented in analogy to what has been done for bosons [43,44]. Moreover, in the recent past several authors (see, e.g., [45,46]) have

proposed to use entanglement measures as a quantum phase transition marker. We think that our model can represent a good test field for this approach to quantum phase transitions.

### APPENDIX A: TUNNELING COEFFICIENT CALCULATION

In the following calculation we will fix  $n_\beta \geq n_\alpha$ , without loss of generality, as can be easily verified.

The integral in Eq. (22) can be decomposed into the sum of three terms

$$\Theta_1^{n_\alpha n_\beta} + \Theta_2^{n_\alpha n_\beta} + \Theta_3^{n_\alpha n_\beta} = \int dy e^{-(y-\tau)^2/2} H_{n_\alpha}(y) - \tau f(y) e^{-y^2/2} H_{n_\beta}(y) \quad (A1)$$

with

$$f(y) = \left( \frac{y^2}{2} - \frac{1 - \cos(2\Omega y)}{4\Omega^2} \right).$$

Integral (A1) is such that

$$\Theta_1^{n_\alpha n_\beta} = - \int \frac{dy}{4\Omega^2} e^{-[y^2+(y-\tau)^2]/2} H_{n_\beta}(y-\tau) H_{n_\alpha}(y), \quad (A2)$$

$$\Theta_2^{n_\alpha n_\beta} = \int \frac{dy}{4\Omega^2} e^{-[y^2+(y-\tau)^2]/2} \cos(2\Omega y) H_{n_\alpha}(y) H_{n_\beta}(y-\tau), \quad (A3)$$

$$\Theta_3^{n_\alpha n_\beta} = \frac{1}{2} \int dy y^2 e^{-[y^2+(y-\tau)^2]/2} H_{n_\alpha}(y) H_{n_\beta}(y-\tau). \quad (A4)$$

The substitution  $\zeta = y - \tau/2$  yields

$$\Theta_1^{n_\alpha n_\beta} = - C_\Omega^\tau \int d\zeta e^{-\zeta^2} H_{n_\alpha}\left(\zeta + \frac{\tau}{2}\right) H_{n_\beta}\left(\zeta - \frac{\tau}{2}\right), \quad (A5)$$

where  $C_\Omega^\tau = e^{-\tau^2/4}/(4\Omega^2)$ . We then use the Hermite polynomial identity

$$H_n(x+y) = \sum_{k=0}^n \binom{n}{k} H_k(x) (2y)^{n-k} \quad (A6)$$

to obtain

$$\begin{aligned} \Theta_1^{n_\alpha n_\beta} = & - \frac{e^{-\tau^2/4}}{4\Omega^2} \int d\zeta e^{-\zeta^2} \sum_{l,k=0}^{n_\alpha n_\beta} \binom{n_\alpha}{l} \binom{n_\beta}{k} \tau^{n_\alpha+n_\beta-(l+k)} \\ & \times (-1)^{n_\beta-k} H_k(\zeta) H_l(\zeta). \end{aligned} \quad (A7)$$

With the orthogonality of Hermite polynomials

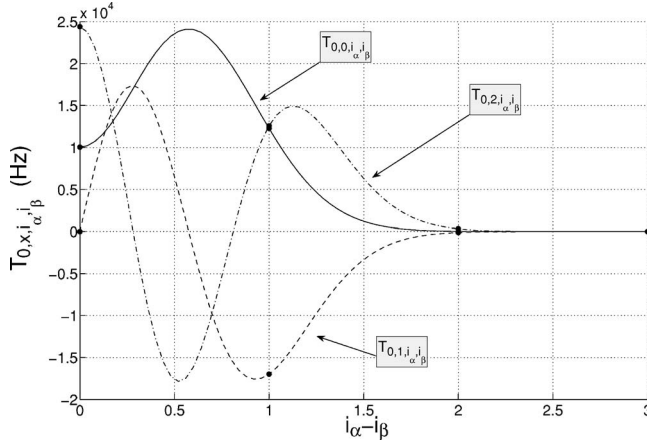


FIG. 3. Plot of  $T_{n_{\alpha}n_{\beta}i_{\alpha}i_{\beta}}$  from  $T_{0,0,i_{\alpha}i_{\beta}}$  to  $T_{0,2,i_{\alpha}i_{\beta}}$ . The solid line represents the case of ground-state tunneling. In this case the hopping parameter  $T_{0,0,i_{\alpha}i_{\beta}}$  is always positive. However, interlevel tunneling already shows sign changes.

$$\int_{-\infty}^{\infty} dx H_n(x)H_m(x)e^{-x^2} = \delta_{n,m}2^n n! \sqrt{\pi} \quad (\text{A8})$$

we are able to perform the  $\zeta$  integration obtaining

$$\Theta_1^{n_{\alpha}n_{\beta}} = -\frac{\sqrt{\pi}}{4\Omega^2} e^{-\tau^2/4} (-1)^{n_{\beta}} \sum_{l=0}^{n_{\alpha}} \binom{n_{\alpha}}{l} \binom{n_{\beta}}{l} \tau^{n_{\beta}+n_{\alpha}-2l} (-2)^l l! \quad (\text{A9})$$

It is worth noting that the summation extends to  $n_{\alpha}$ , that is,  $\binom{a}{b} = 0$  if  $a < b$ . From [37] it can be verified that the last summation is related to generalized Laguerre polynomials, giving

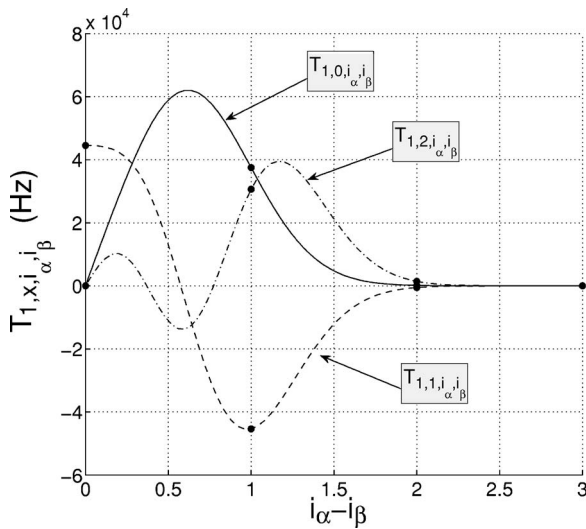


FIG. 4. Plot of  $T_{n_{\alpha}n_{\beta}i_{\alpha}i_{\beta}}$  from  $T_{1,0,i_{\alpha}i_{\beta}}$  to  $T_{1,2,i_{\alpha}i_{\beta}}$ . In this situation the intralevel tunneling term  $T_{1,1,i_{\alpha}i_{\beta}}$  is always negative, but if a different external parameter choice is considered, the sign change can be placed between  $i_{\alpha}-i_{\beta}=1$  and  $i_{\alpha}-i_{\beta}=2$ .

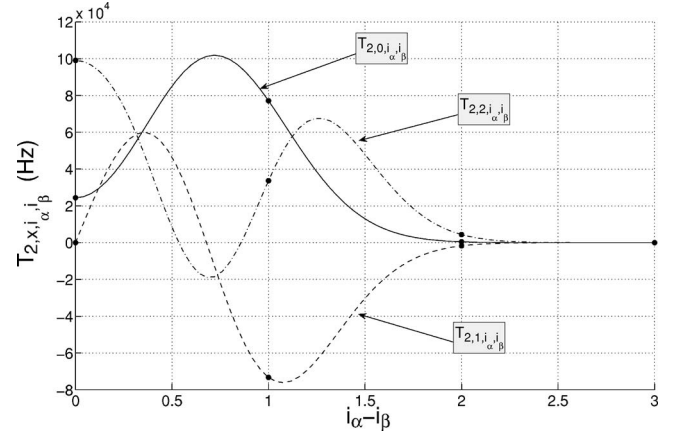


FIG. 5. Plot of  $T_{n_{\alpha}n_{\beta}i_{\alpha}i_{\beta}}$  from  $T_{2,0,i_{\alpha}i_{\beta}}$  to  $T_{2,2,i_{\alpha}i_{\beta}}$ .

$$\Theta_1^{n_{\alpha}n_{\beta}} = -\frac{\sqrt{\pi} n_{\alpha}! 2^{n_{\alpha}}}{4\Omega^2 (-\tau)^{n_{\alpha}-n_{\beta}}} e^{-\tau^2/4} L_{n_{\alpha}}^{n_{\beta}-n_{\alpha}}\left(\frac{\tau^2}{2}\right) \quad (\text{A10})$$

We move now to the calculation of  $\Theta_2^{n_{\alpha}n_{\beta}}$  which is given by

$$\Theta_2^{n_{\alpha}n_{\beta}} = \frac{1}{4\Omega^2} \int dy \exp\left(-\frac{y^2}{2}\right) H_{n_{\alpha}}(y) \exp\left(-\frac{(y-\tau)^2}{2}\right) H_{n_{\beta}}(y - \tau) \cos(2\Omega y) \quad (\text{A11})$$

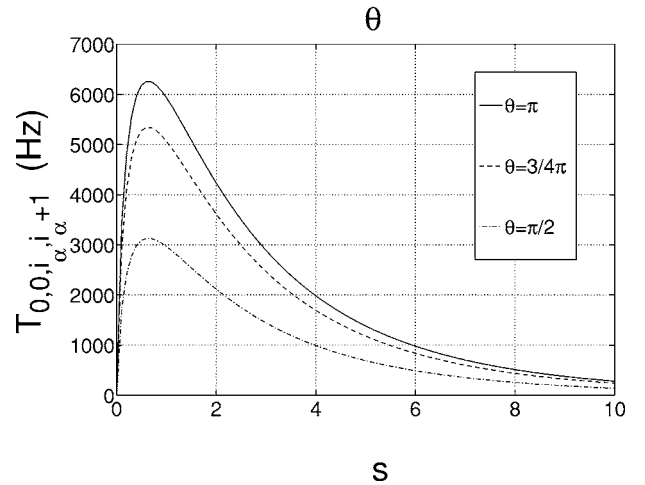
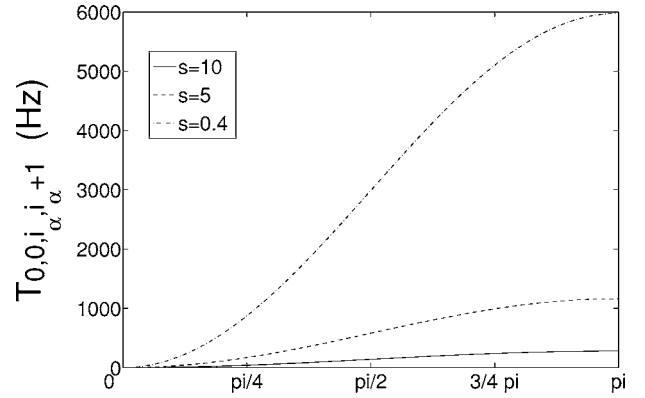


FIG. 6. Plot of  $T_{0,0,i_{\alpha}i_{\beta}+1}$  as a function of  $\theta$  and  $s$ , respectively.

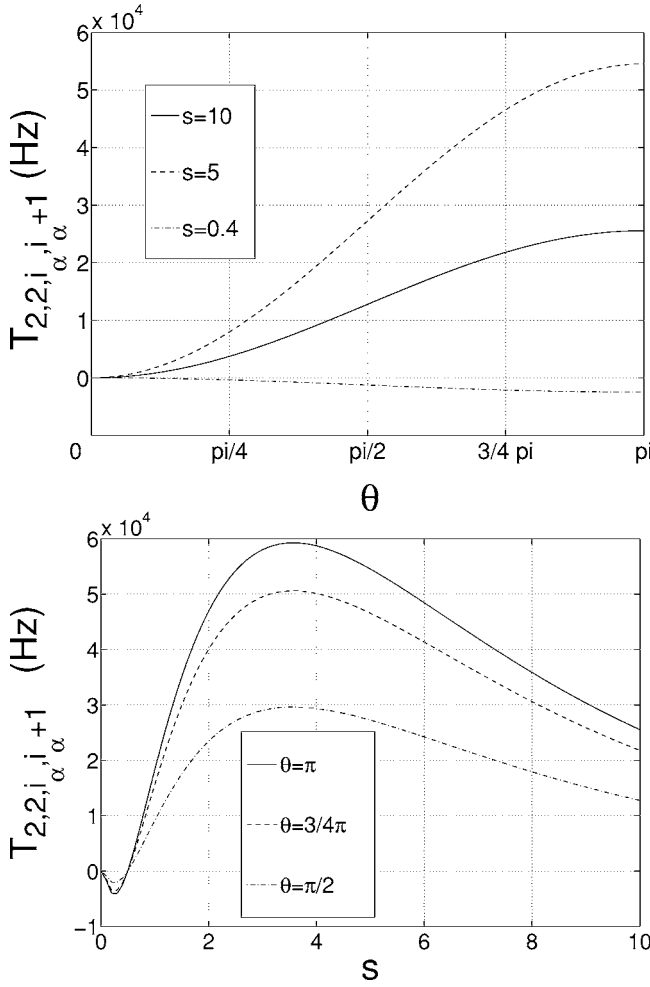


FIG. 7. Plot of  $T_{2,2,i_\alpha,i_\alpha+1}$  as a function of  $\theta$  and  $s$ , respectively. It is worth noticing the region where  $T_{2,2,i_\alpha,i_\alpha+1}$  becomes negative.

Equation (A11), with the substitution  $\zeta=y-\tau/2$ , can be written as

$$\Theta_2^{n_\alpha n_\beta} = \frac{1}{4\Omega^2} \exp(-\tau^2/4) \int d\zeta e^{-\zeta^2} H_{n_\alpha} \left( \zeta + \frac{\tau}{2} \right) H_{n_\beta} \left( \zeta + \frac{\tau}{2} \right) \cos(2\Omega\zeta). \quad (A12)$$

Again, using Eq. (A6) gives

$$\Theta_2^{n_\alpha n_\beta} = \frac{e^{-\tau^2/4} n_\alpha n_\beta}{4\Omega^2} \sum_{l,k=0} \binom{n_\alpha}{l} \binom{n_\beta}{k} \tau^{n_\beta+n_\alpha-(l+k)} \times (-1)^{n_\beta-k} \int d\zeta e^{-\zeta^2} H_k(\zeta) H_l(\zeta) \cos(2\Omega\zeta). \quad (A13)$$

The integral in Eq. (A13) can be interpreted as the real Fourier transform of the function

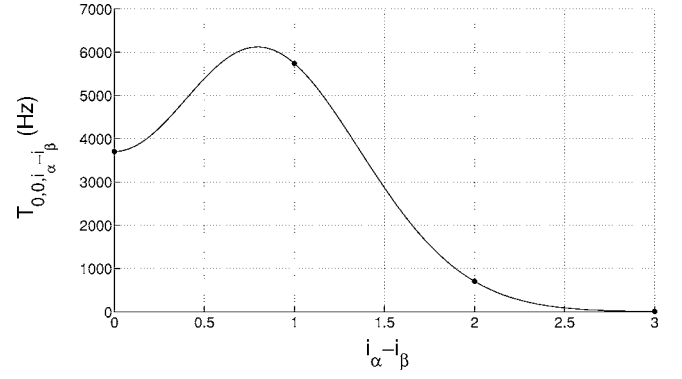


FIG. 8. Plot of  $T_{0,0,i_\alpha,i_\beta}$  for  $s=0.1$ . Next-to-nearest-neighbor hopping parameter differs significantly from zero.

$$e^{-\zeta^2} H_k(\zeta) H_l(\zeta).$$

Recalling that

$$\mathcal{F}[f(x)g(x)] = \mathcal{F}[f(x)] * \mathcal{F}[g(x)],$$

where  $\mathcal{F}[\cdot]$  indicates the Fourier transform and  $*$  the convolution product, we obtain

$$\Theta_2^{n_\alpha n_\beta} = \frac{e^{-\tau^2/4} n_\alpha n_\beta}{4\Omega^2} \sum_{l,k=0} \binom{n_\alpha}{l} \binom{n_\beta}{k} \tau^{n_\beta+n_\alpha-l-k} \times (-1)^{n_\beta-k} \text{Re}\{\mathcal{F}[e^{-\zeta^2/2} H_k(\zeta)] * \mathcal{F}[e^{-\zeta^2/2} H_l(\zeta)]\} \quad (A14)$$

giving

$$\Theta_2^{n_\alpha n_\beta} = \frac{e^{-\tau^2/4} n_\alpha n_\beta}{4\Omega^2} \sum_{l,k=0} \binom{n_\alpha}{l} \binom{n_\beta}{k} \tau^{n_\beta+n_\alpha-(l+k)} (-1)^{n_\beta-k+l} \times \text{Re} \left( i^{k+l} \int d\epsilon e^{-[\epsilon^2+(\epsilon-2\Omega)^2]/2} H_k(\epsilon) H_l(\epsilon-2\Omega) \right). \quad (A15)$$

The integral on the right-hand side of Eq. (A15) can be solved following the same procedure used for  $\Theta_1^{n_\alpha n_\beta}$ :

$$\int d\epsilon e^{-\epsilon^2/2} H_k(\epsilon) e^{-(\epsilon-2\Omega)^2/2} H_l(\epsilon-2\Omega) = (-1)^{k-l} \sqrt{\pi} e^{-\Omega^2} (2\Omega)^{k-l} l! 2^l L_l^{k-l}(4\Omega^2). \quad (A16)$$

Introducing Eq. (A16) in Eq. (A15) gives

$$\Theta_2^{n_\alpha n_\beta} = \frac{e^{-\tau^2/4} n_\alpha n_\beta}{4\Omega^2} \sum_{l,k=0} \binom{n_\alpha}{l} \binom{n_\beta}{k} \tau^{n_\beta+n_\alpha-(l+k)} (-1)^{n_\beta} \times 2^l l! \text{Re}(i^{k+l}) \frac{\sqrt{\pi}}{(2\Omega)^{l-k}} L_l^{k-l}(2\Omega^2) e^{-\Omega^2}. \quad (A17)$$

The calculation of  $\Theta_3^{n_\alpha n_\beta}$  is quite straightforward. Applying twice the identity

$$xH_n(x) = \frac{1}{2}H_{n+1}(x) + nH_{n-1}(x) \quad (\text{A18})$$

we can write  $\Theta_3^{n_\alpha n_\beta}$  as

$$\begin{aligned} \Theta_3^{n_\alpha n_\beta} = \frac{e^{-\tau^2/4}}{2} \int d\zeta e^{-\zeta^2} & \left[ \frac{1}{4}H_{n_\alpha+2}\left(\zeta + \frac{\tau}{2}\right) + \frac{2n_\alpha+1}{2}H_{n_\alpha}\left(\zeta + \frac{\tau}{2}\right) + n_\alpha(n_\alpha-1) \right. \\ & \left. H_{n_\alpha-2}\left(\zeta + \frac{\tau}{2}\right) \right] H_{n_\beta}\left(\zeta - \frac{\tau}{2}\right). \end{aligned} \quad (\text{A19})$$

With the same procedure used for  $\Theta_1^{n_\alpha n_\beta}$ ,  $\Theta_3^{n_\alpha n_\beta}$  is given by

$$\begin{aligned} \Theta_3^{n_\alpha n_\beta} = \frac{(-1)^{n_\beta-n_\alpha}}{2} \sqrt{\pi} 2^{n_\alpha} n_\alpha! \tau^{n_\beta-n_\alpha} e^{-\tau^2/4} & \left[ \frac{(n_\alpha+1)(n_\alpha+2)}{\tau^2} \right. \\ & \times L_{n_\alpha+2}^{n_\beta-n_\alpha-2}(\tau^2/2) + \frac{\tau^2}{4} L_{n_\alpha-2}^{n_\beta-n_\alpha+2}\left(\frac{\tau^2}{2}\right) \\ & \left. + \frac{2n_\alpha+1}{2} L_{n_\alpha}^{n_\beta-n_\alpha}\left(\frac{\tau^2}{2}\right) \right]. \end{aligned} \quad (\text{A20})$$

Hence  $T_{\alpha,\beta}$  becomes

$$T_{\alpha,\beta} = \frac{\hbar\omega_x \delta_{J_\alpha J_\beta} \delta_{m_\alpha m_\beta} \delta_{\sigma_\alpha \sigma_\beta}}{\sqrt{2^{n_\alpha+n_\beta+2} n_\alpha! n_\beta! \pi}} (\Theta_1^{n_\alpha n_\beta} + \Theta_2^{n_\alpha n_\beta} + \Theta_3^{n_\alpha n_\beta}) \quad (\text{A21})$$

with  $\Theta_1^{n_\alpha n_\beta}$ ,  $\Theta_2^{n_\alpha n_\beta}$ , and  $\Theta_3^{n_\alpha n_\beta}$  given by formulas (A10), (A17), and (A20), respectively.

In Figs. 3–5 we plot  $T_{n_\alpha n_\beta i_\alpha i_\beta}$  as a function of the difference  $i_\alpha - i_\beta$  for values of  $n_\alpha$  and  $n_\beta$  ranging from 0 to 2.

The long-distance exponential decay is common to all tunneling coefficients, regardless of the energy level. On the other hand its detailed shape has deep relevance for nearest neighbors and possibly next-to-nearest neighbors (i.e., there may be sign changes passing from  $T_{n,m,i,i+1}$  and  $T_{n,m,i,i+2}$ ) as shown in Figs. 3–8. Another interesting feature is that an extra term, due to “on-site” tunneling coefficients, must be added to the harmonic oscillator energy term.

## APPENDIX B: INTERACTION COEFFICIENTS

We provide here the detailed calculation for the interaction-term matrix elements. To solve integral (27)

$$\begin{aligned} U_x = \frac{1}{\pi l_x} \sqrt{\frac{2^{-(n_\alpha+n_\beta+n_\gamma+n_\delta)}}{n_\alpha! n_\beta! n_\gamma! n_\delta!}} \\ \times \int dx H_{n_\alpha}(x) H_{n_\beta}(x) H_{n_\gamma}(x) H_{n_\delta}(x) e^{-2x^2}, \end{aligned}$$

we exploit again Eq. (A6), obtaining

$$\begin{aligned} U_x = \frac{1}{\pi l_x} \sqrt{\frac{2^{-(n_\alpha+n_\beta+n_\gamma+n_\delta)}}{n_\alpha! n_\beta! n_\gamma! n_\delta!}} \sum \binom{n_\alpha}{i_\alpha} \binom{n_\beta}{i_\beta} \binom{n_\gamma}{i_\gamma} \\ \times \binom{n_\delta}{i_\delta} H_{i_\alpha}(0) H_{i_\beta}(0) H_{i_\gamma}(0) H_{i_\delta}(0) \\ \times \int d\zeta (2\zeta)^{n_\alpha+n_\beta+n_\gamma+n_\delta-(i_\alpha+i_\beta+i_\gamma+i_\delta)} e^{-2\zeta^2}. \end{aligned} \quad (\text{B1})$$

In the previous equation the summation must be intended over four independent values of  $s_\theta=0, \dots, n_\theta$  with  $\theta=\alpha, \beta, \gamma, \delta$ . With the substitution

$$\int d\zeta (2\zeta)^\alpha e^{-2\zeta^2} = \delta_{\alpha,2N} \sqrt{2}^{\alpha-3} \Gamma[(\alpha+1)/2] \quad (\text{B2})$$

( $\delta_{\alpha,2N}$  indicates that  $\alpha$  must be an even number) Eq. (B1) becomes

$$U_x = \frac{1}{\pi l_x} \sum_{\vec{s}} \frac{\Xi(\vec{s})}{\sqrt{2^{|\vec{s}|+3}}} \Gamma\left(\frac{\|\vec{s}\| - \|\vec{s}\| + 1}{2}\right) \delta_{\|\vec{s}\|, 2N} \quad (\text{B3})$$

with

$$\vec{a} = \{a_\alpha, a_\beta, a_\gamma, a_\delta\} \quad \left(1 - \text{norm } \|\vec{a}\| = \sum_\theta a_\theta\right) \quad (\text{B4})$$

and

$$\Xi(\vec{s}) = \prod_\theta \frac{1}{\sqrt{n_\theta!}} \binom{n_\theta}{s_\theta} H_{s_\theta}(0), \quad (\text{B5})$$

where  $\Xi(\vec{s})=0$  for odd  $i_\theta$ . The  $\delta$  function in Eq. (B3) should be written as  $\delta_{\|\vec{s}\|-\|\vec{s}\|, 2N}$ . However, the condition  $\|\vec{s}\|=\text{even}$  already implies  $\|\vec{s}\|=\text{even}$ . We are then allowed to write  $\delta_{\|\vec{s}\|-\|\vec{s}\|, 2N} = \delta_{\|\vec{s}\|, 2N}$  in Eq. (B3).

We solve now the radial part of the interaction-term integral written in Eq. (30),

$$U_\rho = \int \int \frac{d^2\eta}{\pi} \mathcal{L}_{J_\alpha m_\alpha}^*(\eta) \mathcal{L}_{J_\gamma m_\gamma}^*(\eta) \mathcal{L}_{J_\beta m_\beta}(\eta) \mathcal{L}_{J_\delta m_\delta}(\eta),$$

where  $\eta=(\rho, \phi)$  and  $d^2\eta=\rho d\rho d\phi$ . Following [37], we express  $\mathcal{L}_{J_\alpha m_\alpha}(\rho, \phi)$  in terms of a finite sum

$$\begin{aligned} \mathcal{L}_{J_\alpha m_\alpha}(\rho, \phi) = e^{2im_\alpha\phi} e^{-\rho^2/l_\perp^2} \sqrt{(J_\alpha+m_\alpha)! (J_\alpha-m_\alpha)!} \\ \times \frac{1}{\pi} \sum_{q_\alpha=|m_\alpha|}^{J_\alpha} \frac{(-1)^{J_\alpha-q_\alpha} (\rho/l_\perp)^{2q_\alpha}}{(J_\alpha-q_\alpha)! (q_\alpha+m_\alpha)! (q_\alpha-m_\alpha)!}. \end{aligned} \quad (\text{B6})$$

Hence the radial part of  $\mathcal{L}_{J_\alpha m_\alpha}(\vec{\rho}, \phi)$  can be written as

$$R_{J_\alpha m_\alpha}(\vec{\rho}) = \frac{e^{-(\vec{\rho}/l_\perp)^2/2}}{l_\perp} \sum_{q_\alpha=|m_\alpha|}^{J_\alpha} \Lambda_\alpha(\vec{\rho}/l_\perp)^{2q_\alpha}, \quad (\text{B7})$$

where

$$\Lambda_\alpha = \frac{(-1)^{J_\alpha-q_\alpha} \sqrt{(J_\alpha+m_\alpha)! (J_\alpha-m_\alpha)!}}{(J_\alpha-q_\alpha)! (q_\alpha+m_\alpha)! (q_\alpha-m_\alpha)!}. \quad (\text{B8})$$

Substituting Eq. (B7) into Eq. (30) we have

$$U_\rho = \frac{2\delta_{m_\alpha+m_\gamma, m_\beta+m_\delta}}{\pi l_\perp^4} \sum_{q_\alpha=|m_\alpha|}^{J_\alpha} \sum_{q_\beta=|m_\beta|}^{J_\beta} \sum_{q_\gamma=|m_\gamma|}^{J_\gamma} \sum_{q_\delta=|m_\delta|}^{J_\delta} \times \Lambda_\alpha \Lambda_\beta \Lambda_\gamma \Lambda_\delta \int_0^\infty d\rho \frac{\rho}{\pi l_\perp^2} \left(\frac{\rho}{l_\perp}\right)^{2\|\bar{q}\|} e^{-2\bar{\rho}^2} \quad (\text{B9})$$

$$U_\rho = \frac{\delta_{m_\alpha+m_\gamma, m_\beta+m_\delta}}{\pi l_\perp^2} \sum_{\bar{q}=|m|}^{\bar{J}} \Lambda(\bar{J}, \bar{m}, \bar{q}) \frac{\Gamma(\|\bar{q}\| + 3/2)}{2^{\|\bar{q}\|+3/2}} \quad (\text{B10})$$

with

$$\Lambda(\bar{J}, \bar{m}, \bar{q}) = \prod_{\theta=\alpha, \beta, \gamma, \delta} \Lambda_\theta. \quad (\text{B11})$$

which, with the same notation of Eq. (B3), becomes

- 
- [1] M. H. Anderson, J. R. Ensher, M. R. Matthews, C. E. Wieman, and E. A. Cornell, *Science* **269**, 198 (1995).
- [2] K. B. Davis, M.-O. Mewes, M. R. Andrews, N. J. van Druten, D. S. Durfee, D. M. Kurn, and W. Ketterle, *Phys. Rev. Lett.* **75**, 3969 (1995).
- [3] A. J. Leggett, *Rev. Mod. Phys.* **73**, 307 (2001).
- [4] F. Dalfovo, S. Giorgini, L. P. Pitaevskii, and S. Stringari, *Rev. Mod. Phys.* **71**, 463 (1999).
- [5] D. Jaksch and P. Zoller, *Ann. Phys. (N.Y.)* **31**, 52 (2005).
- [6] L. P. Pitaevskii and S. Stringari, *Bose-Einstein Condensation* (Oxford Science, Oxford, 2003).
- [7] B. Anderson and M. Kasevich, *Science* **282**, 1686 (1998).
- [8] C. Orzel, A. Tuchman, M. Y. M. Feneslau, and M. A. Kasevich, *Science* **291**, 2386 (2001).
- [9] O. Morsch, J. H. Muller, M. Cristiani, D. Ciampini, and E. Arimondo, *Phys. Rev. Lett.* **87**, 140402 (2001).
- [10] D. Jaksch, C. Bruder, J. I. Cirac, C. W. Gardiner, and P. Zoller, *Phys. Rev. Lett.* **81**, 3108 (1998).
- [11] P. Buonsante, V. Penna, and A. Vezzani, *Phys. Rev. A* **70**, 061603(R) (2004).
- [12] P. Buonsante and A. Vezzani, *Phys. Rev. A* **70**, 033608 (2003).
- [13] S. Peil, J. V. Porto, B. L. Tolra, J. M. Obrecht, B. E. King, M. Subbotin, S. L. Rolston, and W. D. Phillips, *Phys. Rev. A* **67**, 051603(R) (2003).
- [14] L. Guidoni and P. Verkerk, *Phys. Rev. A* **57**, R1501 (1998).
- [15] R. Roth and K. Burnett, *Phys. Rev. A* **68**, 023604 (2003).
- [16] L. Santos, M. A. Baranov, J. I. Cirac, H.-U. Everts, H. Fehrmann, and M. Lewenstein, *Phys. Rev. Lett.* **93**, 030601 (2004).
- [17] S. J. J. M. F. Kokkelmans, J. N. Milstein, M. L. Chiofalo, R. Walser, and M. J. Holland, *Phys. Rev. A* **65**, 053617 (2002).
- [18] P. Rabl, A. J. Daley, P. O. Fedichev, J. I. Cirac, and P. Zoller, *Phys. Rev. Lett.* **91**, 110403 (2003).
- [19] J. N. Milstein, S. J. J. M. F. Kokkelmans, and M. J. Holland, *Phys. Rev. A* **66**, 043604 (2002).
- [20] L. Giorgetti, L. Viverit, G. Gori, F. Barranco, E. Vigezzi, and R. A. Broglia, *J. Phys. B* **38**, 949 (2005).
- [21] M. Greiner, C. Regal, and D. S. Jin, *Nature (London)* **426**, 537 (2003).
- [22] G. E. Astrakharchik, J. Boronat, J. Casulleras, and S. Giorgini, *Phys. Rev. Lett.* **93**, 200404 (2004).
- [23] T. Calarco, U. Dorner, P. Julienne, C. Williams, and P. Zoller, *Phys. Rev. A* **70**, 012306 (2004).
- [24] P. Zanardi, *Phys. Rev. A* **65**, 042101 (2002).
- [25] W. Greiner, *Quantum Mechanics: Special Chapters* (Springer-Verlag, Berlin, 1998).
- [26] A. A. Abrikosov, *Methods of Quantum Field Theory in Statistical Physics* (Dover Publications, New York, 1977).
- [27] G. Modugno, G. Roati, F. Riboli, F. Ferlaino, R. Brecha, and M. Inguscio, *Science* **297**, 2240 (2002).
- [28] L. Pezzé, L. Pitaevskii, A. Smerzi, S. Stringari, G. Modugno, E. De Mirandes, F. Ferlaino, H. Ott, G. Roati, and M. Inguscio, *Phys. Rev. Lett.* **93**, 120401 (2004).
- [29] W. Hofstetter, J. I. Cirac, P. Zoller, E. Demler, and M. D. Lukin, *Phys. Rev. Lett.* **89**, 220407 (2002).
- [30] A. Albus, F. Illuminati, and J. Eisert, *Phys. Rev. A* **68**, 023606 (2003).
- [31] S. R. Granade, M. E. Gehm, K. M. O'Hara, and J. E. Thomas, *Phys. Rev. Lett.* **88**, 120405 (2002).
- [32] S. M. Giampaolo, F. Illuminati, G. Mazzarella, and S. De Siena, *Phys. Rev. A* **70**, 061601(R) (2004).
- [33] V. Bach, E. Lieb, and J. Solovej, *J. Stat. Phys.* **76**, 3 (1994).
- [34] W. Zhang, D. Feng, and R. Gilmore, *Rev. Mod. Phys.* **62**, 867 (1990).
- [35] G. Modugno, F. Ferlaino, R. Heidemann, G. Roati, and M. Inguscio, *Phys. Rev. A* **68**, 011601(R) (2003).
- [36] Kerson Huang, *Statistical Mechanics* (Wiley, New York, 1987).
- [37] A. Wünsche, *J. Phys. A* **31**, 8267 (1998).
- [38] V. Ruuska and Törmä, *New J. Phys.* **6**, 59 (2004).
- [39] G. Roati, F. Riboli, G. Modugno, and M. Inguscio, *Phys. Rev. Lett.* **88**, 150403 (2002).
- [40] A. Montorsi, M. Rasetti, and A. I. Solomon, *Phys. Rev. Lett.* **59**, 2243 (1987).
- [41] A. Montorsi and V. Penna, *Phys. Rev. B* **60**, 12069 (1999).
- [42] S. R. White, *Phys. Rev. B* **48**, 10345 (1993).
- [43] G. G. Batrouni, R. T. Scalettar, G. T. Zimanyi, and A. P. Kampf, *Phys. Rev. Lett.* **74**, 2527 (1995).
- [44] J. K. Freericks and H. Monien, *Phys. Rev. B* **53**, 2691 (1996).
- [45] C. Yan, P. Zanardi, Z. Wang, and F. C. Zhang, e-print quant-ph/0407228.
- [46] R. Somma, G. Ortiz, H. Barnum, E. Knill, and L. Viola, *Phys. Rev. A* **70**, 042311 (2004).